

INTERNATIONAL THERMONUCLEAR EXPERIMENTAL REACTOR

ITER EDA NEWSLETTER

VOL.9, No. 10

OCTOBER 2000

INTERNATIONAL ATOMIC ENERGY AGENCY, VIENNA, AUSTRIA

ISSN 1024-5642

SPECIAL ISSUE

OUTLINE OF THE NEW ITER DESIGN

by Dr. R. Aymar, ITER Director

The next step on the path towards establishing fusion as a practical long-term energy source, with acceptable environmental characteristics, is to construct and operate a burning plasma experiment that allows, in one device, full exploration of the physics issues as well as proof of principle and testing of key technological features of possible fusion power stations. ITER would provide the basis for the design of a first demonstration fusion power station that would demonstrate the reliable generation of electricity, before a prototype power plant could be envisaged for commercial use on competitive grounds.

In July 1998 the ITER Parties were unable, for financial reasons, to proceed to construction of the design proposed at that time to meet the detailed technical objectives and target cost set in 1992. It was therefore decided to investigate options for the design of ITER with reduced technical objectives and with possibly decreased technical margins, whose target construction cost was half that of the previous design, while maintaining the overall programmatic objective.

The revised performance specifications for ITER adopted by the Parties in June 1998 (as reported in previous Newsletters), require, in summary:

- to achieve extended burn in inductive operation with $Q \geq 10$, not precluding ignition, with an inductive burn duration between 300 and 500 s, a 14 MeV average neutron wall load $\geq 0.5 \text{ MW/m}^2$, and a fluence $\geq 0.3 \text{ MWa/m}^2$;
- to aim at demonstrating steady state operation using non-inductive current drive with $Q \geq 5$;
- to use, as far as possible, technical solutions and concepts developed and qualified during the EDA;
- to target about 50% of the direct capital cost of the 1998 ITER design with particular attention devoted to cash flow.

To identify designs that might meet the revised objectives, task forces involving the JCT and Home Teams met during 1998 and 1999 to analyse and compare a range of options for the design of such a device. Using the common vehicle of system codes to consistently relate the main plasma parameters, physics design constraints, engineering features, and costs, along with more detailed studies of engineering and physics aspects of specific cases, representative options that span an appropriate range of aspect ratio were selected for further elaboration and more comprehensive consideration. This led at the end of 1999 to a single configuration for the ITER design with parameters considered to be the most credible consistent with technical limitations and the financial target, yet meeting fully the objectives with appropriate margins.

The new design of ITER, called "ITER-FEAT", was submitted by the ITER Director to the ITER Parties as the "ITER FEAT Outline Design Report" in January 2000, at their Meeting in Tokyo. The Parties subsequently conducted their domestic assessments of this report and fed the resulting comments back into the progressing design. The progress on the developing design was reported to TAC in June 2000 in the report "Progress in Resolving Open Design Issues from the ODR" alongside a status report on validating R&D. The design was subsequently approved by the governing body of ITER in Moscow in June 2000 as the basis for the preparation of the Final Design Report, recognising it as a single mature design for ITER consistent with its revised objectives. This article summarizes the main design features - further details can be found in ITER EDA Documentation Series No. 19, IAEA, Vienna.

The main plasma parameters and overall dimensions are summarised in Table 1. The figures show parameters and dimensions for nominal operation; figures in brackets represent maximum values under specific limiting conditions, including, in some cases, additional capital expenditures.

Table 1. Main Plasma Parameters and Dimensions

Total Fusion Power	500 MW (700 MW)
Q-Fusion power/auxiliary heating power	10
Average Neutron Wall loading	0.57 MW/m ² (0.8 MW/m ²)
Plasma inductive burn time	300 s.
Plasma major radius	6.2 m
Plasma minor radius	2.0 m
Plasma current (I _p)	15 MA (17.4 MA)
Vertical elongation @95% flux surface/separatrix	1.70/1.85
Triangularity @95% flux surface/separatrix	0.33/0.49
Safety factor @95% flux surface	3.0
Toroidal field @ 6.2 m radius	5.3 T
Plasma Volume	837 m ³
Plasma Surface	678 m ²
Installed Auxiliary Heating/Current Drive power	73 MW (100 MW)

A cross-section of the tokamak showing the vacuum vessel, its internal components and its ports, as well as some features of the magnet system and cryostat, is shown in Figure 1. Figure 2 shows an overall schematic of systems important for normal operation. Further details of the physics basis and performance, and engineering design, are given in the Annexes. The assessment by each Party recognises the feasibility of the design to meet its objectives, the adequacy of the margins that remain against the uncertainties, and recognises the sufficient underpinning of the design by the R&D database.

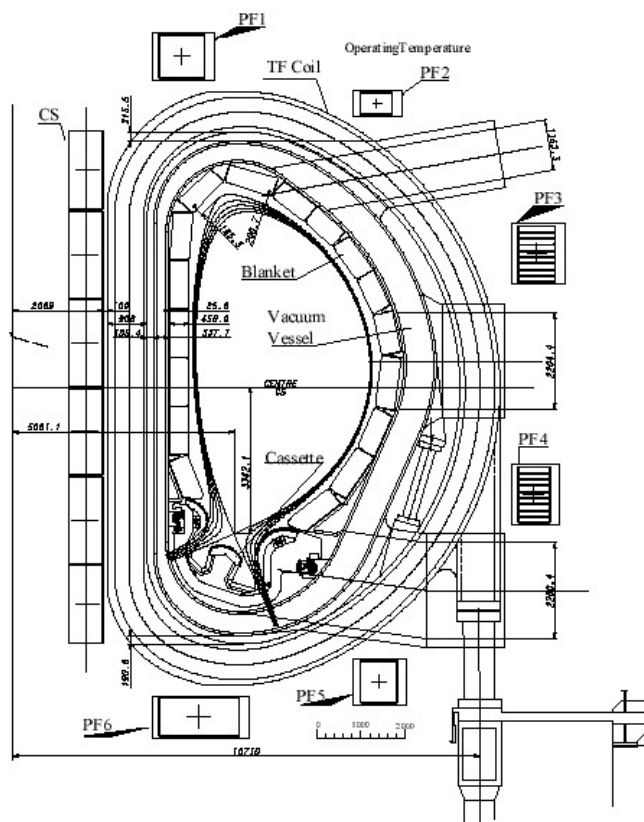


Figure 1. Cross-Section of the Tokamak

With regard to safety and licensing issues, the current design focuses on confinement as the overriding safety function of equipment, the others being recognised as being required to protect confinement. A "lines-of-defence" methodology is to obtain the required level of safety while balancing the requirements imposed on systems and components. The number and quality of the lines of defence then depend on the inventory at risk.

Concerning cost, the previous 1998 ITER design cost understanding has been used as fully as possible to estimate the cost of the new design, including all construction, operating and decommissioning costs. The simple scalings used cannot take into account design improvements that have also occurred in the interim, which gives confidence that the resulting estimate, which is 56% of the cost of the 1998 ITER design, can be improved on in the more realistic estimates that are being produced in late 2000 by the Parties' laboratories and industries based on "procurement packages" - draft technical specifications consistent with a plausible procurement contract, including technical descriptions and drawings, and indicating the apportioning of responsibilities for performance between ITER and the potential supplier, in order to prepare for contract quotation.

Regarding schedule, construction is now envisaged to require just over 8 years from the license to construct until the first plasma. For operation, the early years envisage a period of simulation of fusion performance using only hydrogen plasmas, before the machine becomes activated in DT operations. A typical scenario envisages nominal DT shots in the 5th year of operation, for instance, with progressively higher duty factor thereafter.

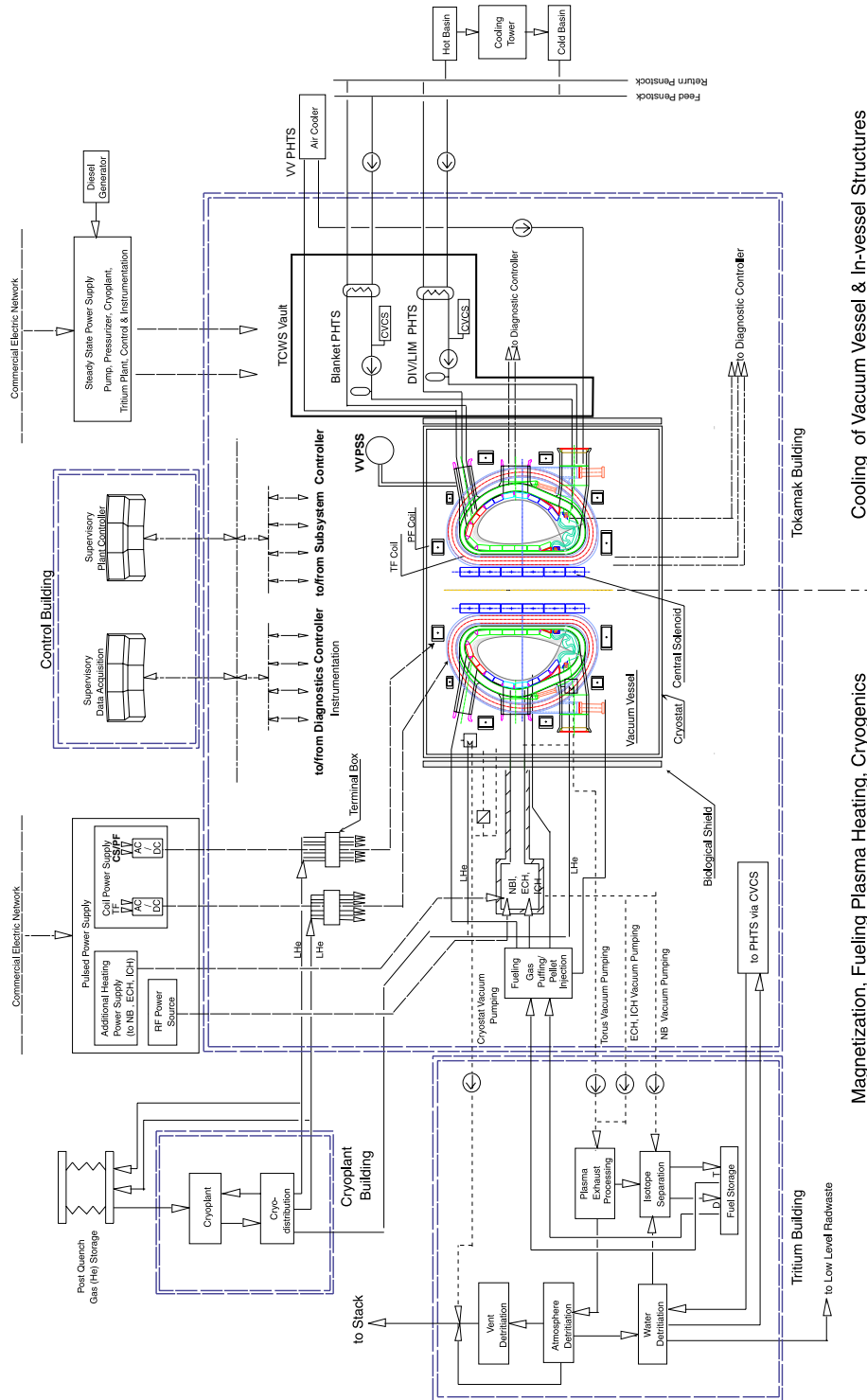


Figure 2. Plant Systems Diagram

Physics Basis and Plasma Performance Projections

The reference operating scenario for inductive operation is the ELMy H-mode and the rules and methodologies for projection of plasma performance to the ITER scale are those established in the ITER Physics Basis (IPB)*), which has been developed from broadly-based experimental and modelling activities within the magnetic fusion programmes of the ITER Parties.

The key physics issues relating to plasma performance in the ELMy H-mode regime are:

- the maintenance of H-mode quality confinement at sufficiently high density, achieving adequate plasma β to produce the requisite fusion power, and hence Q value;
- the provision of satisfactory power and particle exhaust by the divertor to ensure acceptable levels of helium and plasma impurities;
- the evolution of plasma confinement phenomena scaling with size;
- efficient transfer of α -particle power to the thermal plasma while limiting anomalous α -particle losses, via TF ripple or collective instabilities, to prevent damage to the plasma facing components.

At the same time, global magnetohydrodynamic (mhd) stability and plasma control capability must be such that the thermal and electromagnetic loads, as well as runaway electron currents, arising from disruptions are within acceptable bounds.

H-mode operation at high plasma density is favoured by the choice of a high plasma triangularity and the exploitation of high-field-side ('inside') fuel pellet launch, while the overall choice of design parameters allows considerable headroom for Q=10 operation well below the Greenwald density. Optimum use of the plasma pressure for fusion power production implies that densities in the vicinity of (and, in power plants, perhaps beyond) the Greenwald density $n_{GW} (10^{20} m^{-3}) = I_p (MA)/p^2(m)$ be attained. Plasma performance predictions show that Q=10 operation can be achieved at modest values of β_N (~1.5). However, in the event that the b threshold for the onset of neoclassical tearing modes (NTMs) scales unfavourably with size, stabilization of the modes by localized ECCD is foreseen.

Extensive divertor model validation and analysis activities performed so far during the EDA give confidence that the proposed divertor design allows adequate power dissipation to be achieved, with peak power loads below the acceptable level of $10 MW m^{-2}$, and that the planned fuelling throughput of $200 Pam^{-3}s^{-1}$ will limit the core helium concentration below 6%.

The essential physics which enters into the prediction of plasma performance in ITER derives from the two principal ELMy H-mode scalings, i.e. the H-mode power threshold scaling, which defines the lower boundary of the device operating window in terms of fusion power, and the energy confinement time scaling. The recommended form for the former scaling is,

$$P_{LH} = 2.84 M^{-1} B_T^{0.82} n_e^{0.58} R^{1.00} a^{0.81} \quad (\text{rms err. } 0.268)$$

in (MW, AMU, T, $10^{20} m^{-3}$, m), with M the effective isotopic mass of the plasma fuel, and for the latter the IPB98(y,2) scaling,

$$\tau_{E,th}^{IPB98(y,2)} = 0.0562 H_H I_p^{0.93} B_T^{0.15} P^{-0.69} n_e^{0.41} M^{0.19} R^{1.97} \varepsilon^{0.58} \kappa_x^{0.78} \quad (\text{rms err. } 0.145)$$

where the units are (s, MA, T, MW, $10^{19} m^{-3}$, AMU, m) and the elongation k_a is defined as $k_a = S_0/(pa^2)$ with S_0 being the plasma cross-sectional area. The enhancement factor H_H measures the quality of confinement ($<$ or >1). A comparison of the H-mode thermal confinement times with the scaling for a subset of ELMy data in the ITER H-mode database is shown in Figure A1-1.

Because the simultaneous choice of non-dimensional parameters ($A = R/a$, k , d , q_{95} , β_N , n/n_{GW}) which, when close to their respective limits, may have some significant hidden interactions which affects the energy confinement, other methods have been pursued to establish confidence in the performance predicted for ITER-FEAT. They extrapolate pulses from present experiments keeping all these parameters constant, merely scaling the size until criteria of energy multiplication or power are satisfied. In accordance with this alternative design methodology, the ITER-FEAT design seems to be soundly based on the extrapolation of high performance ELMy H-mode shots from JET, JT-60, DIII-D, and ASDEX-U.

*) ITER Physics Basis, *Nuclear Fusion* 39 (1999) 2175

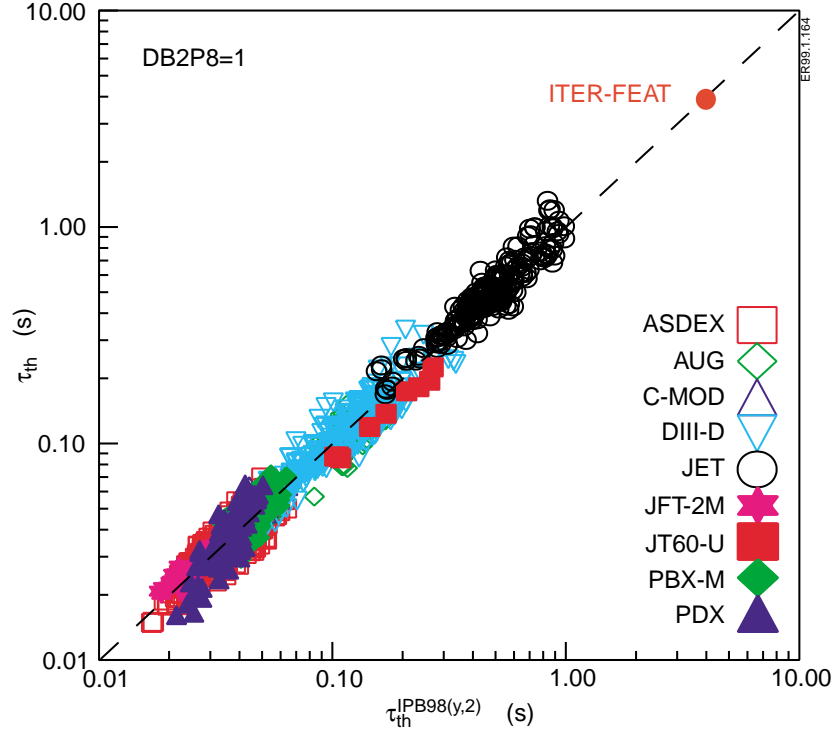


Figure A1-1. Comparison of ELMy H-mode thermal energy confinement times with the scaling expression $IPB98(y,2)$ and scaling prediction for the energy confinement time in a nominal inductive $Q=10$ discharge.

To illustrate the range of performance which can be achieved in ITER-FEAT, Figure A1-2 shows values of P_{fus} and Q as a function of the auxiliary heating power for discharges with $I_p = 13.1, 15.1$ and 17.4 MA in which an operating point having $H_H = 1$ and $n/n_{GW} = 0.85$ is selected. The minimum fusion power at 15.1 and 13.1 MA is limited by the L-H back transition, taken as $1.3P_{LH}$.

A more complete view of the range of plasma parameters at which $Q=10$ operation is possible can be gained from an analysis of the operational domain in terms of fusion power and H_H , in which the various operational boundaries ($P_{loss} = 1.3P_{LH}$, $n = n_{GW}$, and $\beta_N = 2.5$) can also be traced, as shown in Figure A1-3 and -4. Inside the indicated domain $Q=10$ is maintained, but the auxiliary power is adjusted together with the density.

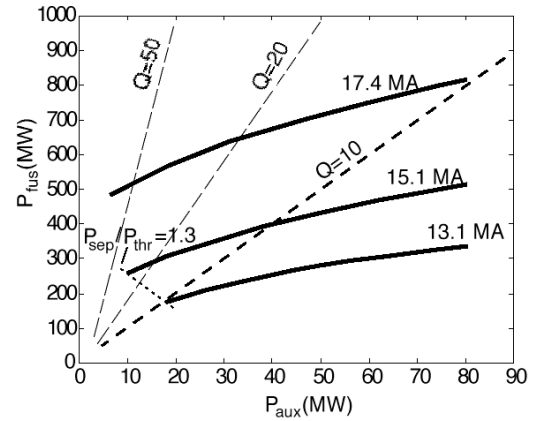


Figure A1-2. P_{fus} as a function of P_{aux} for $I = 13.1, 15.1$ and 17.4 MA at $H_H = 1$ and $n/n_{GW} = 0.85$.

The results illustrate the flexibility of the design, its capacity for responding to factors which may degrade confinement while maintaining its goal of extended burn $Q=10$ operation, and, by implication, its ability to explore higher Q operation as long as energy confinement times consistent with the confinement scaling are maintained.

The capability of the ITER design for steady-state operation with $Q=5$ are being studied numerically using 0-dimensional analysis within the limitations of current assumptions. Two operational scenarios are under consideration for steady-state operation: high current (12 MA) with monotonic q or shallow shear, and modest current (9 MA) with negative shear. The high current steady-state operation requires all the current drive power (100 MW) available, but the requirements on confinement ($H_H \sim 1.2$) and beta ($\beta_N \sim 3$) are modest. On the other hand, the low current steady-state operation requires more challenging values of confinement improvement $H_H \sim 1.5$ and beta ($\beta_N \sim 3.2-3.5$). Performance predictions for these modes of operation are much less certain than for inductive operation. In particular, the operating space is sensitive to assumptions about current drive efficiency and plasma profiles.

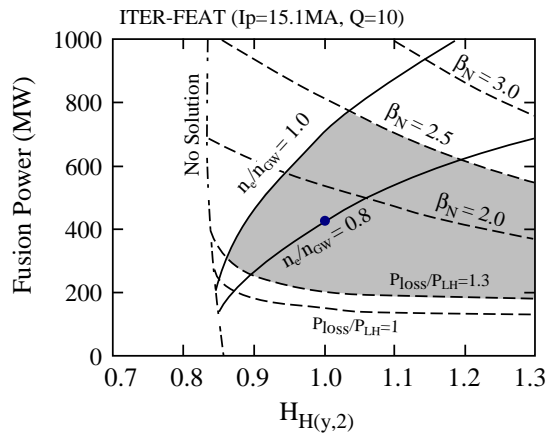


Figure A1-3 $Q = 10$ domain (shaded) for $I_p = 15.1$ MA ($q_{95} = 3.0$).

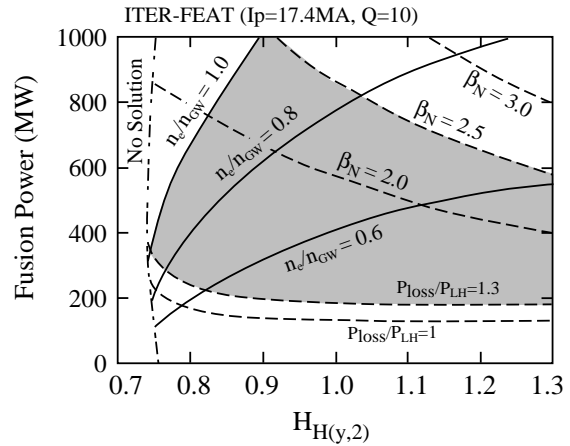


Figure A1-4 $Q = 10$ domain (shaded) for $I_p = 17.4$ MA ($q_{95} = 2.6$).

In addition, the potential performance of hybrid modes of operation, where, in addition to inductively driven current, a substantial fraction of the plasma current is driven by external heating and the bootstrap effect leading to extension of the burn duration, is being evaluated as a promising route towards establishing true steady-state modes of operation. This form of operation would be well suited to systems engineering tests.

An operation space, in terms of fusion power versus confinement enhancement factor, and showing the transition from hybrid to true steady-state operation is illustrated in Figure A1-5 for $I_p = 12$ MA and $P_{CD} = 100$ MW. For a given value of fusion power (and hence Q), as the confinement enhancement factor, H_H , increases (simultaneously decreasing plasma density and increasing β_N), the plasma loop voltage falls towards zero. For example, operation with $V_{loop} = 0.02$ V and $I_p = 12$ MA, which corresponds to a flat-top length of 2500 s, is expected at $H_H = 1$, $Q = 5$, $n_e/n_{GW} = 0.7$, and $\beta_N = 2.5$. True steady-state operation at $Q = 5$ can be achieved with $H_H = 1.2$ and $\beta_N = 2.8$. This analysis indicates that a long pulse mode of operation is accessible.

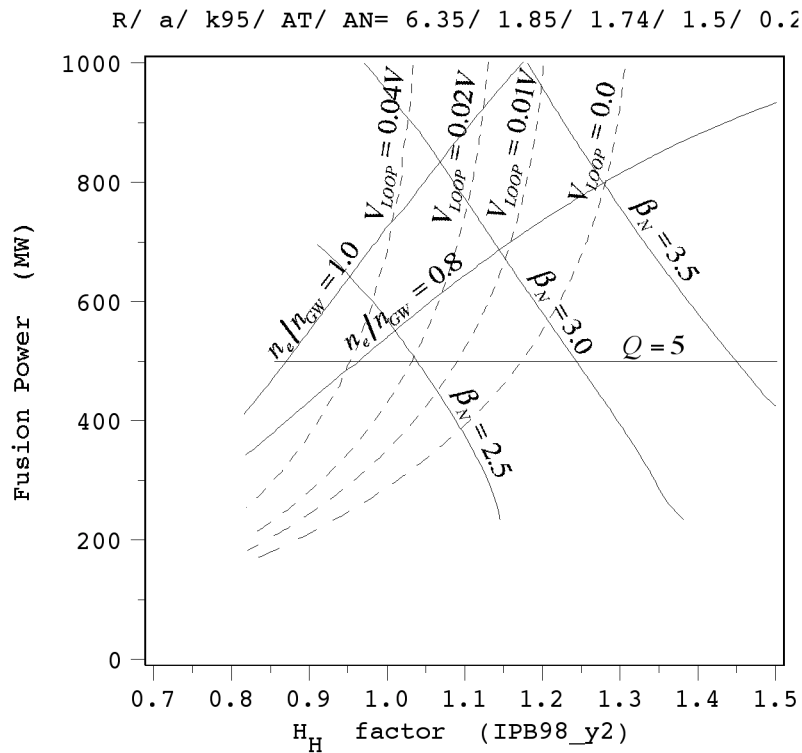


Figure A1-5 . Operation space for hybrid (long pulse) and steady-state operation. Here, $I_p = 12$ MA and $P_{CD} = 100$ MW.

Design Features and Assessments

The design of ITER-FEAT uses as far as possible technical solutions and concepts developed and qualified during the EDA so far. Nonetheless, changes in overall scale and in some physics requirements (e.g. more plasma shaping); the pressure to preserve the plasma performance capacity and flexibility, whilst approaching the 50% cost target, have induced some significant changes in the design features from the 1998 ITER Design and, in addition, the continuing flow of new data from the technology R&D has enabled changes to be made in design associated with a better knowledge of the available margins.

The main engineering features and materials in the design are summarised in Table A2-1. Because of the unwillingness to compromise with physics extrapolation so as to provide enough margins in the physical parameters and physics-related systems e.g., plasma size, fuelling, and heating and current drive, a major focus of effort is to press on the manufacturing processes (with their feedback on design) to approach as closely as possible the target of 50% saving in direct capital cost from the 1998 ITER design.

Table A2-1. Main Engineering Features of ITER

Superconducting toroidal field coils (18 coils) Superconductor Structure	Nb ₃ Sn in circular stainless steel (SS) jacket in grooved radial plates Pancake wound, in welded SS case, wind, react and transfer technology	
Superconducting Central Solenoid (CS) Superconductor Structure	Nb ₃ Sn in square Incoloy jacket, or in circular Ti/SS jacket inside SS U-channels Pancake wound, 3 double or 1 hexa-pancake, wind react and transfer technology	
Superconducting poloidal field coils (PF 1-6) Superconductor Structure	NbTi in square SS conduit Double pancakes	
Vacuum Vessel (9 sectors) Structure Material	Double-wall welded ribbed shell, with internal shield plates and ferromagnetic inserts SS 316 LN structure, SS 304 with 2% boron shield, SS 430 inserts	
First Wall/Blanket (421 modules) Structure Materials	(Initial DT Phase) Single curvature faceted separate FW attached to shielding block which is fixed to vessel Be armour, Cu-alloy heat sink, SS 316 LN structure	
Divertor (54 cassettes) Configuration Materials	Single null, cast or welded plates, cassettes W alloy and C plasma facing components Copper alloy heat sink, SS 316 LN structure	
Cryostat Structure Maximum inner dimensions Material	Ribbed cylinder with flat ends 28 m diameter, 24 m height SS 304L	
Heat Transfer Systems (water-cooled) Heat released in the tokamak during pulsed operation	nominal	750 MW at 3 and 4.2 MPa water pressure, ~120°C
Cryoplant Nominal average He refriger. /liquefac. rate for magnets & divertor cryopumps (4.5K) Nominal cooling capacity of the thermal shields at 80 K	55 kW / 0.13 kg/s	
	660 kW	
Additional Heating and Current Drive Total injected power Candidate systems	73 MW initially, 100 MW nominal maximum Electron Cyclotron, Ion Cyclotron, Lower Hybrid, Negative Ion Neutral Beam	
Electrical Power Supply Pulsed Power supply from grid Total active/reactive power demand Steady-State Power Supply from grid Total active/reactive power demand	500 MW / 400 MVar	
	110 MW/ 78 MVar	

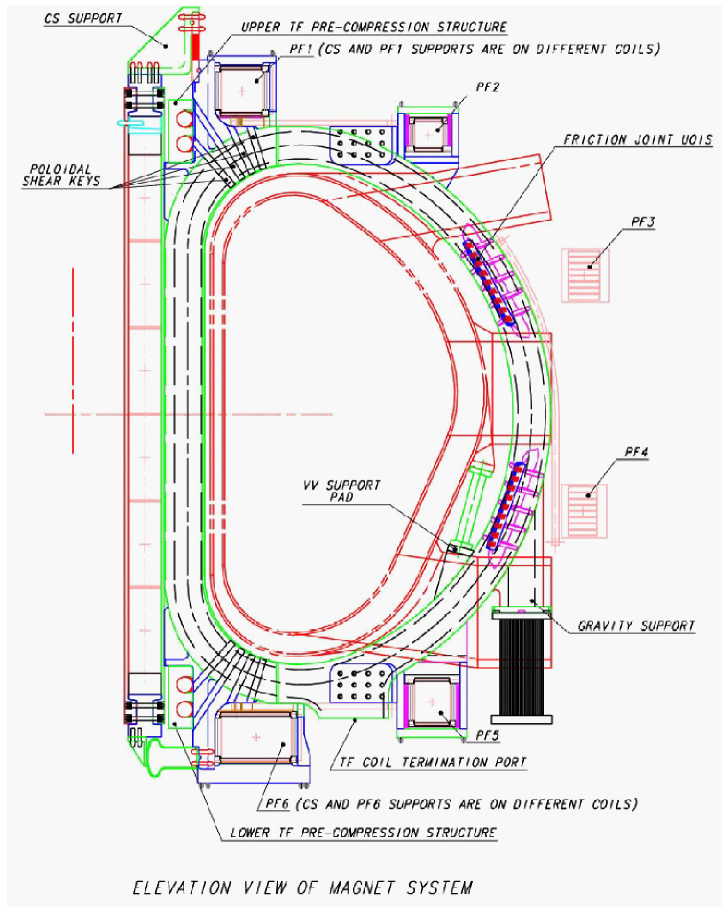
The following paragraphs summarise and assess the key features of the ITER-FEAT components and subsystems, and the overall plant systems integration.

Magnets and structures

The superconducting magnet system which confines, shapes and controls the plasma inside a toroidal vacuum vessel comprises three main systems and their power supplies:

- 18 Toroidal Field (TF) coils which produce the confining/stabilizing toroidal field;
- 6 Poloidal Field (PF) coils which contribute to the plasma positioning and shaping;
- a Central Solenoid (CS) coil which provides the main contribution to inducing current in the plasma.

Correction coils (including three sets located above, outboard of and below the TF coils) are also required to correct error fields that arise due to imperfections in the actual PF and TF coil configuration and to stabilize the plasma against resistive wall mode instabilities.



The magnet system weighs, in total, about 8,700 t - about one third of the weight of the 1998 design.

The CS and TF coils use Nb_3Sn as superconductor, and the technology of "wind, react and transfer", whereas the PF and correction coils use NbTi. All coils are cooled by supercritical helium at $\sim 4.5\text{K}$. The TF coil case is the main structural component of the magnet system and the machine core. The PF coils and vacuum vessel are linked to the TF coils such that all interaction forces are resisted internally in the system. The TF coil inboard legs are wedged all along their side walls in operation and they are all linked at their two ends to two strong coaxial rings which provide toroidal compression and resist the local de-wedging of those legs under load. At the outboard leg, the out-of-plane support is provided by intercoil structures integrated with the TF coil cases. Views of the magnet system are shown in Figure A2-1.

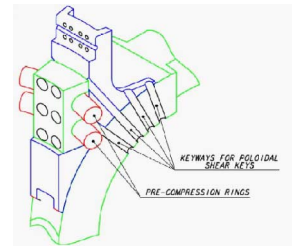


Figure A2-1. Magnet System

Two options were considered for the TF coil winding: one with a circular conductor embedded in radial plates and the other with a square conductor. The radial plate option was selected due to the greater insulation reliability, despite cost and radial build penalties.

For the CS winding, which is free-standing and thus subject to two load cycles per pulse, there are two options to provide the structural material which is subject to fatigue due to the large number of pulses. The first one uses an Incoloy square jacket with a co-wound strip and the second one uses two, stainless steel, U-channels welded (after the heat treatment to react the Nb and Sn) around a thin circular, jacket made of titanium. The selection of the option can be postponed until more R&D results are available.

In total, the results from the large scale R&D (e.g. tests of the CS model coil) provide confidence that the remaining issues for the magnet design are not ones of feasibility or performance but, rather, issues which relate to manufacturing options to reduce the capital cost.

The whole tokamak (vacuum vessel, magnet and associated structures) is located within a single-walled cryostat and within the cryostat there are thermal shields at 80K to prevent the cold portions ($\sim 4\text{K}$) from receiving heat from the

“hotter” parts. Bellows are used to connect the interspace duct wall extensions of the VV ports with the cryostat port to compensate for differential movements.

Liquid helium from a cryoplant is distributed by a cryodistribution system to auxiliary cold boxes feeding the magnet and other loads (e.g. cryopumps for the pumping of the vacuum vessel). Circulating pumps force the flow of supercritical helium through the load in each separate circuit, which exchanges heat with a helium bath, whose pressure (and thus temperature) are controlled by a cold compressor in the return path towards the cryoplant. The plant design reconciles the pulsed character of the heat deposited in the magnet coils and the cryopumps, with the steady operation of the cryorefrigerator, which handles only the average heat load.

Although the envisaged cryoplant is a very large and complex facility, the confidence of building such a plant with the required performance is very high since the cryorefrigerator and cryodistribution systems for large particle accelerators provide good bases that can be directly applied to the ITER-FEAT system design.

Vacuum Vessel, Blanket and Divertor

The double-walled vacuum vessel is lined by modular removable components, including blanket modules composed of a separate first wall mounted on a shield block, divertor cassettes, and diagnostics sensors, as well as port plugs such as the limiter, heating antennae, and test blanket modules. All these removable components are mechanically attached to the VV. These vessel and internal components absorb most of the radiated heat from the plasma and protect the magnet coils from excessive nuclear radiation. This shielding is accomplished by a combination of steel and water, the latter providing the necessary removal of heat from absorbed neutrons. A tight fitting configuration of the VV to the plasma aids the passive plasma vertical stability, and ferromagnetic material in the VV located under the TF coils reduces the TF ripple. The overall arrangement of one of the 9 vacuum vessel sectors is shown in Figure A2-2.

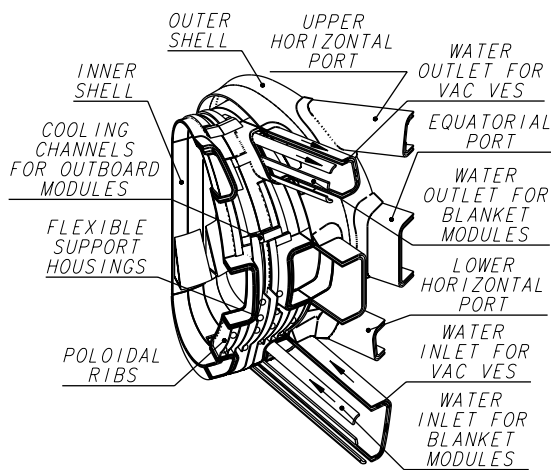


Figure A2-2.
Vacuum Vessel Overall Arrangement

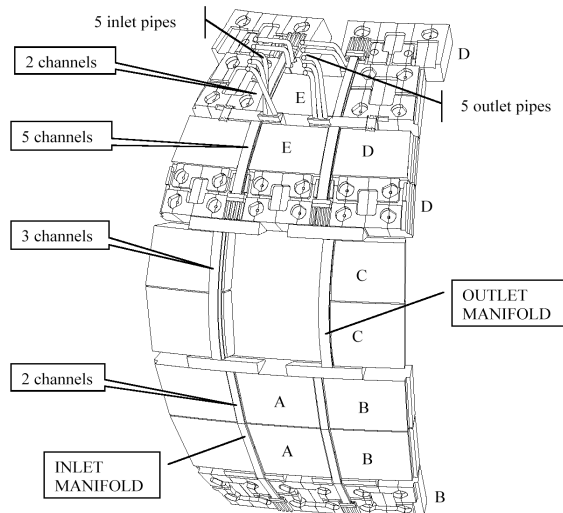


Figure A2-3.
Blanket Module Cooling Arrangement

The initial blanket acts solely as a neutron shield, and tritium breeding experiments are confined to the test blanket modules which can be inserted and withdrawn at radial equatorial ports. The blanket module design consists of a separate faceted first wall (FW) built with a Be armour and a water cooled copper heat sink attached to a SS shielding block. This minimises radioactive waste and simplifies manufacture.

Two options were considered for blanket cooling: one with cooling channels integrated inside the vessel structure between the two walls, the other with channels mounted on the vessel in vacuum. The latter (Figure A2-3) has been selected based on its greater robustness and relative ease of manufacture, as well as the significantly reduced complexity in the design of the vessel, which is the primary confinement boundary.

The manufacture of a full-scale vacuum vessel sector, and the manufacture and testing of blanket and FW mockups, of the 1998 ITER design gives a sound basis for the present design. To reduce the VV fabrication cost, forging, powder HIPing and/or casting is being investigated for the large number of the housings in the VV for the blanket module support that have a relatively small and simple structure.

The divertor is made up of 54 cassettes. Figure A2-4 shows the V-shaped configuration of the target and divertor floor and the large opening between the inner and outer divertor legs to allow an efficient exchange of neutral particles. These choices provide a large reduction in the target peak heat load, without adversely affecting helium removal.

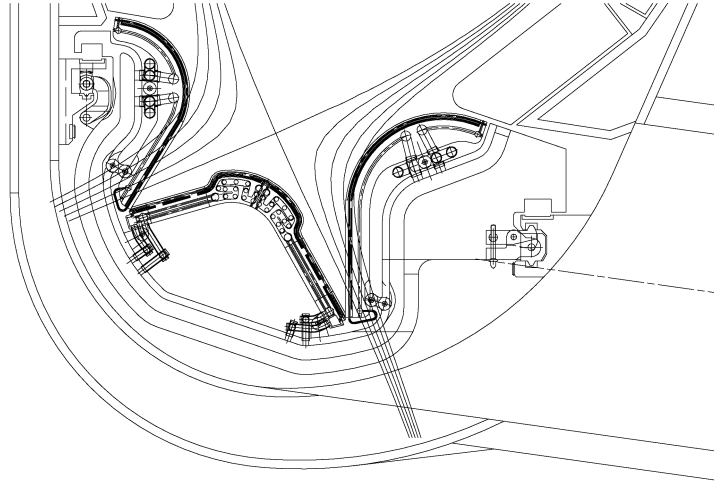


Figure A2-4 Divertor Plasma Facing Components Arrangement

The current design uses carbon at the vertical target strike points. Tungsten is being considered as a backup, and both materials have their advantages and disadvantages. The two options need continuous development so that the best judgement of the relative merits can be made by the time of procurement. Carbon has the best behaviour to withstand large power density pulses (ELMs, disruptions), but gives rise to tritiated dust. Procedures for the removal of tritium codeposited with carbon by a number of schemes are under consideration and need further development.

The development of carbon and tungsten armoured plasma facing components has advanced to a level capable of meeting the demanding requirements of the divertor for the average target heat load. The armour behaviour against large power density pulses (such as those arising from large negative edge-localised modes) could be the limiting factor. A successful R&D campaign has demonstrated that armoured components can routinely operate with heat loads of up to 20 MW/m^2 for carbon and $> 10 \text{ MW/m}^2$ for tungsten, with a promise of also reaching 20 MW/m^2 . A prototypical armoured vertical target, which is compatible with the divertor requirements, has been built and fully tested. Furthermore, successful operation in tokamaks, with the scrape-off layer partially detached from the divertor targets, has demonstrated that the average heat flux to the divertor can be reduced through radiation to a larger surrounding area to a value where the armour lifetime is adequate. This is the basis for confidence in the design.

The fuelling and pumping system also provides plasma density control. The tokamak fuelling system is capable of gas puffing and pellet injection into the plasma. Excess fuel gases are subsequently removed from the plasma together with the helium ash using the torus cryopumps, which exhaust to the tritium plant where impurities are removed from the hydrogen stream and the various isotopes of hydrogen are separated and stored. The tritium plant also detritiates water and ventilation air.

Many subsystems in the ITER tritium plant are based on proven, industrial processes at relevant scale. In some instances the dynamic nature of ITER operation requires additional confirmation and this is targeted by R&D, e.g., on the isotope separation system and hydrogen storage beds. Overall there is confidence that, given the expected outcome of the R&D, the necessary subsystems can be procured and operated as required.

The heat deposited in the vessel-internal components and the vessel is rejected to the environment via the tokamak cooling water system, which is designed to preclude releases of tritium and activated corrosion products to the environment. Natural convection in the vessel is able to exhaust their decay heat and keep components well below the temperature at which there is no significant chemical reaction between steam (air) and Be-dust.

Heating and Current Drive

The H&CD systems under consideration for ITER are shown in Table A2-2.

Table A2-2. Heating and Current Drive Systems

	NB	EC (170 GHz)	ICRF (~ 50 MHz)	LH (5 GHz)
Power injected per unit equatorial port (MW)	16.5	20	20	20
Number of units for the first phase	2	1	1	0
Total power (MW) for the first phase	33	20	20	0
The 20 MW of EC module power will be use either i) in 2 upper ports to control neoclassical tearing modes at the $q = 3/2$ and $q = 2$ magnetic surfaces, or ii) in one equatorial port for H&CD mainly in the plasma centre.				

Whilst the designs draw, in general, on existing operational systems, all the options require further R&D to validate the designs and to ensure the performance targets, in the conditions foreseen only for ITER. If reasonable R&D programmes are maintained to address the various issues, the required range of heating and current drive capacity can be made available.

Diagnostics

A large number of special diagnostics will be applied to the tokamak to measure various properties of the confined plasma, the confining magnetic field and the fusion reaction products. Some of these diagnostics are not only required to evaluate the experiments but are required for machine protection (e.g. to avoid excessive heat loads on vessel-internal surfaces and the consequent damage), and for plasma control (e.g. magnetic field measurements which are required for the control of the plasma shape and position by the PF coils).

Key issues are lifetime of components exposed to significant radiation damage, such as magnetic pickups, windows and mirrors, and the desired angle of view to provide the necessary resolution, e.g. neutron cameras and active charge exchange systems. Although further work is required, R&D results encourage the view that viable design solutions exist. Most of the measurements required for the machine protection and basic plasma control can be made using established techniques.

Buildings and Services

The above systems are housed within buildings and structures along with plant services. Considerable effort has been made to make the best use of building space while providing an optimised layout for the required performance of the plant at a minimum cost. For ease of construction, the tokamak and its closely associated systems are located mainly in the lower areas of the buildings as illustrated in Figure A2-5 which shows a section through the tokamak building.

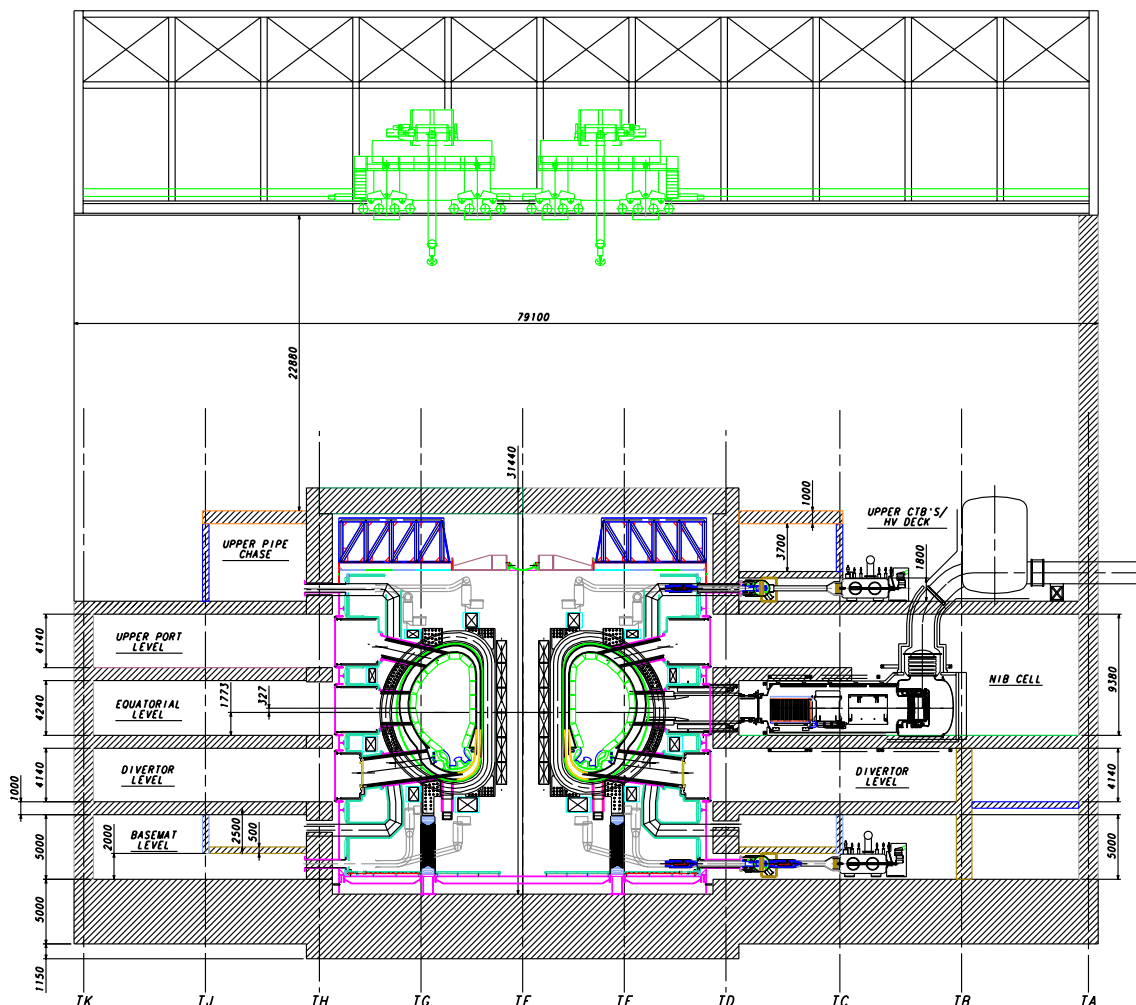


Figure A2-5. Tokamak Building North-South Section

Tokamak Maintenance

Systems near the plasma will become radioactive and will require remote maintenance, with special remote handling equipment. An in-vessel transporter system is used for the removal and reinstallation of blanket modules, multifunction manipulators for divertor cassette removal, and specialised manipulators to handle vacuum vessel port plugs. Special casks, which dock horizontally to the access ports of the vacuum vessel, are designed to house such equipment and to transport radioactive items from the tokamak to the hot-cell where refurbishment or waste disposal operations can be carried out. Docking of these casks to the vessel and the hot cell flanges is tight, to avoid spreading of contamination. Hands-on assisted maintenance is used wherever justifiable, following the ALARA principles.

The remote handling strategy for ITER has been confirmed by a comprehensive R&D programme which has successfully demonstrated that key maintenance operations such as blanket and divertor replacement can be achieved using common remote handling technology. Several crucial issues such as vacuum vessel remote cutting and re-welding, viewing, materials and components radiation hardness have been addressed and demonstrated. In new studies, the possibility of adopting a compact hot cell design based on refurbishing the divertor cassettes and diagnostics during the maintenance period looks promising and is being further assessed.

Overall, the development programme results so far obtained indicate that the remote maintenance strategy for ITER is sound and sufficiently mature to support ITER operation.

Plant control system

The control system consists of a centrally-positioned supervisory control system (SCS) and sub-control systems dedicated to each plant subsystem under the supervision of the SCS. Individual plant and diagnostic subsystems are directly controlled and monitored by their own dedicated intelligent control system. All systems use the same control method of conditional transitions between well-defined steps (i.e. SFC - Sequential Functional Control). The SCS controls the transition of the entire ITER plant from one operation state to another, and provides high level commands to plant subsystems, in order to achieve integrated control of the entire plant. The SCS also monitors the operation state of each plant subsystem to ensure it is operating within its proper operational envelope.

An interlock system monitors operational events of the plant, and performs preventive and protective actions to maintain the system components in a safe operating condition. The interlock system is also hierarchically structured and has individual interlock subsystems which are dedicated to each plant subsystem under the central supervisory interlock system.

The control system for ITER follows well-established principles of system control. Accordingly, no major problems are expected in implementing the design.

Items to be considered for inclusion in the ITER Newsletter should be submitted to B. Kuvshinnikov, ITER Office, IAEA, Wagramer Strasse 5, P.O. Box 100, A-1400 Vienna, Austria, or Facsimile: +43 1 2633832, or e-mail: c.basaldella@iaea.org (phone +43 1 260026392).

Printed by the IAEA in Austria
September 2000